Electronic Supplementary Material (ESI) for Nanoscale.

Electronic Supplementary Information: Finding the true pathway for reversible isomerization of a single azobenzene molecule tumbling on Au(111) surface

Zhen Xie,[a,b] Sai Duan,*[c] Chuan-Kui Wang,[a] and Yi Luo*[b,d]

S1 Computational details

All calculations were performed in the framework of DFT by using the Vienna ab initio simulation package.[1] In present simulations of the adsorbed azobenzene (AB) molecule on Au(111), periodic boundary condition model was adopted. We employed the Perdew-Burke-Ernzerhof (PBE) generalized gradient approximation (GGA) exchange–correlation functional[2] with a 400 eV cutoff of plane-wave and projector augmented-wave pseudopotentials.[3,4] Van der Waals interactions were included by Grimme's empirical correction (D3) with Becke-Jonson damping.[5,6] The atomic structures were relaxed until the forces on all unconstrained atoms were less than 0.02 eV/Å for geometry optimization. Spin unpolarized method was adopted.

The calculated lattice constant of Au was 4.146 Å, agreeing well with the experimental value of 4.086 Å.[7] Three layers of $(5\sqrt{3}\times6)$ supercells of the Au(111) slab were used to simulate the Au surface. For the k-point sampling, a $2\times2\times1$ mesh of the Monkhorst-Pack grid[8] was used. Along the z axis in the supercell, enough vacuum layer ($>$ 35 Å) was added, and the dipole correction[9,10] was used to avoid the artificial interactions. All constant current STM images were calculated within the Tersoff–Hamann approximation.[11] It notes that the prerequisite for Tersoff–Hamann model is no substantial overlap between surface and tip.[12] As a result, the resistance across the tunneling junction should be more than 100 MΩ.[13] This condition is totally fulfilled because the estimated resistance is around 10^4 MΩ in experiments.[14] The energy window was set to 1.0 eV above the Fermi level, which is consistent with the experimental setup.[14] The isovalue was set to 1.0×10^{-5} e/Å^3 and the final STM images were filtered by the Gaussian smoothing with bandwidth of 1.0 Å. The calculated local electron density of states (LDOS) is used to simulate the normalized conductance $(\mathrm{dI/dV})/(\mathrm{I/V})$, *i.e.*, the scanning tunneling spectroscopy (STS).[14,15] The theoretical LDOS spectrum was convoluted by the Lorentzian function with fwhm of 0.04 eV. The climbing-image nudged elastic band method was applied to locate the transition state with eight images.[16] During relaxations for geometry and reaction pathway optimizations, two bottom layers of the substrate were fixed to mimic the Au bulk while all other atoms are allowed to relax. The reaction pathway was optimized until the forces acting on the path were converged typically less than 0.05 eV/Å, and the shapes of the energy curves were determined from the gradient of each image. Furthermore, for frequency calculations, we used the central finite difference with 0.01 Å in displacement in the case of fixing all substrate atoms. Zero point energies (ZPE) were calculated with small negative modes excluded from the summation.

---

[a] Shandong Province Key Laboratory of Medical Physics and Image Processing Technology, School of Physics and Electronics, Shandong Normal University, Jinan 250014, People's Republic of China.

[b] Department of Theoretical Chemistry and Biology, School of Engineering Sciences in Chemistry, Biotechnology and Health, KTH Royal Institute of Technology, S-106 91 Stockholm, Sweden.

[c] Collaborative Innovation Center of Chemistry for Energy Materials, Shanghai, Key Laboratory of Molecular Catalysis and Innovative Materials, MOE Key Laboratory of Computational Physical Sciences, Department of Chemistry, Fudan University, Shanghai 200433, People's Republic of China. E-mail: duansai@fudan.edu.cn

[d] Hefei National Laboratory for Physical Science at the Microscale and Synergetic Innovation Center of Quantum Information & Quantum Physics, University of Science and Technology of China, Hefei, 230026 Anhui, People's Republic of China. E-mail: yiluo@ustc.edu.cn

S2 Zero point energy contribution to azobenzene stability

Table S1 Without (ΔE) and with (ΔE_{ZPE}) zero point energy corrected relative energies for different structures with respect to *trans* configuration adsorbed on Au(111).

	ΔE in eV	ΔE_{ZPE} in eV
trans	0.000	0.000
TS1	1.113	1.100
$cis-$down	0.826	0.835
$cis-$para	1.112	1.104
TS2	1.896	1.872
$cis-$up	1.305	1.278

S3 Additional theoretical STM results as well as simulated details of STM height profiles

To simulate the experimental STM height profile of *cis*-AB, ellipse was used to fit the STM image owing to the oval shape of the experimental and calculated STM images as shown in Fig. S6. The ratio of the major and minor axes of the fitted ellipse for experimental STM image is 1.30, comparing to that of 1.33 for simulated *cis*-up STM image, as well as 1.51 for simulated *cis*-para STM image. It finds that for the experimental result, the angle α between the major axis of the ellipse and the dashed white line that used for corresponding STM height measurement is 17°. As a result, same vale of angle α was adopted in the STM height profiles for *cis*-up and *cis*-para configurations (Fig. S6). In practical simulations, the well-understood *trans*-AB configuration provides a criterion for matching the simulated STM height profiles with experimental results for *cis*. We note that in the Tersoff-Hamann approximation, there are many effects on the corrugation amplitude in STM simulations.[17,18] Among them, the most significant effect is the underestimated band gap predicted by GGA functionals, which would drag more diffuse unoccupied molecular orbitals into the bias window. As a result, the corrugation amplitude could be overestimated, which leads to scaling factors less than 1.0. Specifically, the height profile of *trans*-AB well resembles its experimental counterpart with a scale factor of 0.80 modulated in the calculated height (Fig. S2). As a result, the same scale factor of 0.80 was used to simulate the STM height profile for *cis*-up (Fig. 3d, in the main text). However, the calculated height was scaled by the factor of 0.71 for *cis*-para (Fig. 2c, in the main text) to capture the autofit comparability with the experimental observation. We want to stress that the scale factor was only used for theoretical STM height profile to match the absolute value measured in experiments, and no scale factor was applied for theoretical STM image because it is the contrast that matters the imaging.

The Gaussian function with the form $y = y_0 + \frac{a}{w} e^{-4ln2(\frac{x-b}{w})^2}$ is used to fit the simulated STM height profile of Fig. 2c and Fig. 3d in the main text, aiming at a quantitative comparison with the experimental measurement. Here, the height contribution was calculated by the parameter of $\frac{a}{w}$, and y_0 comes from the background. The parameter w is the full width at half maximum (FWHM), and b represents the position of the center of the peak. All parameters that used to mimic the lines in Fig. S7 and Fig. S10 were summarized in Table S2.

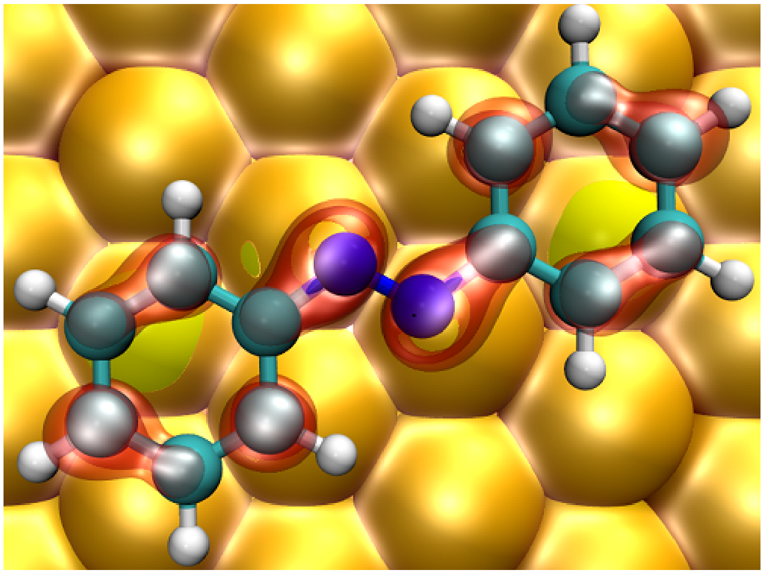

Fig. S1 Isosurface with the value of 0.01 e/Å^3 (red) of the density of states under experimental positive 1.0 V sample bias for *trans* molecule adsorbed on the Au(111) surface.

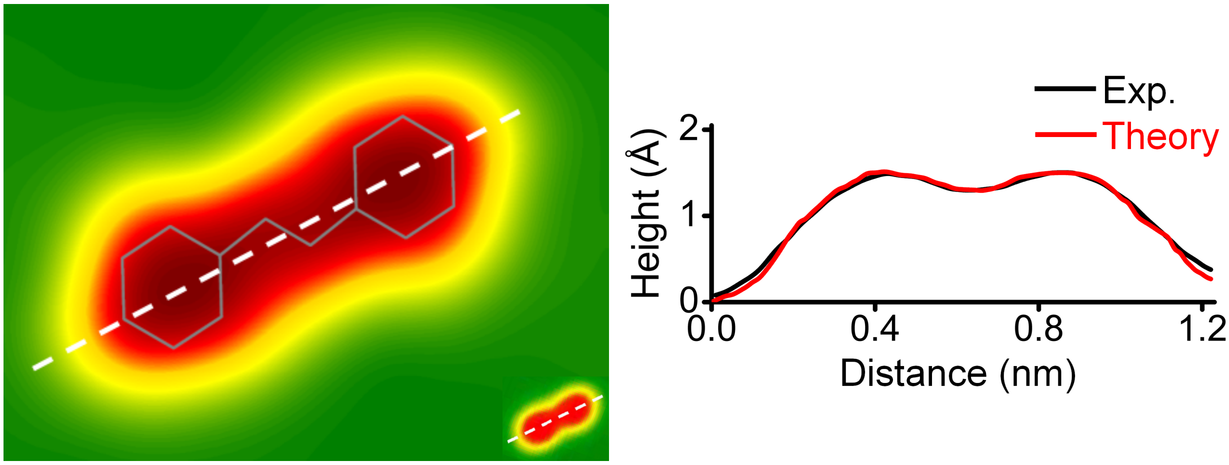

Fig. S2 Calculated STM image in the left panel with the positive sample bias 1.0 V for *trans* configuration, and the experimental STM image is inset. Calculated (red line) and experimental (black line) STM height profiles in the right panel along the dashed white lines marked in the calculated and experimental STM images, respectively. Both experimental STM image and height profile are extracted from Ref. 14.

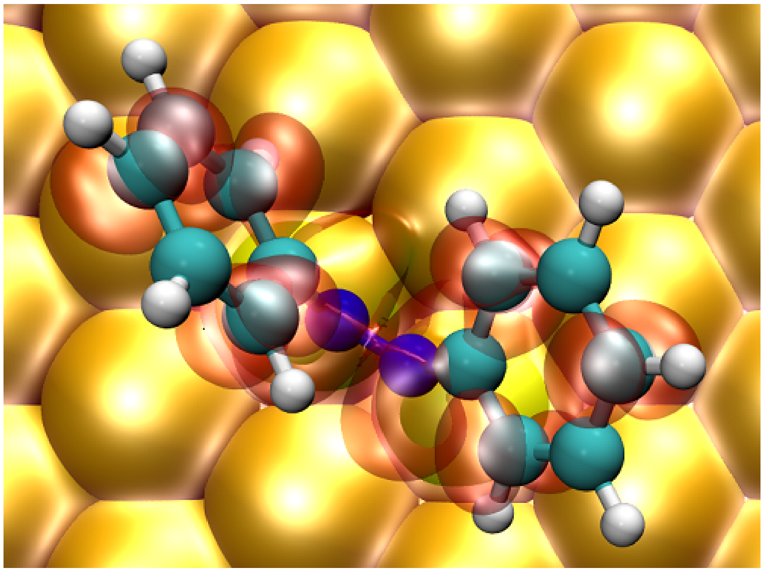

Fig. S3 Isosurface with the value of 0.008 e/Å^3 (red) of the density of states under experimental positive 1.0 V sample bias for *cis*-down molecule adsorbed on the Au(111) surface.

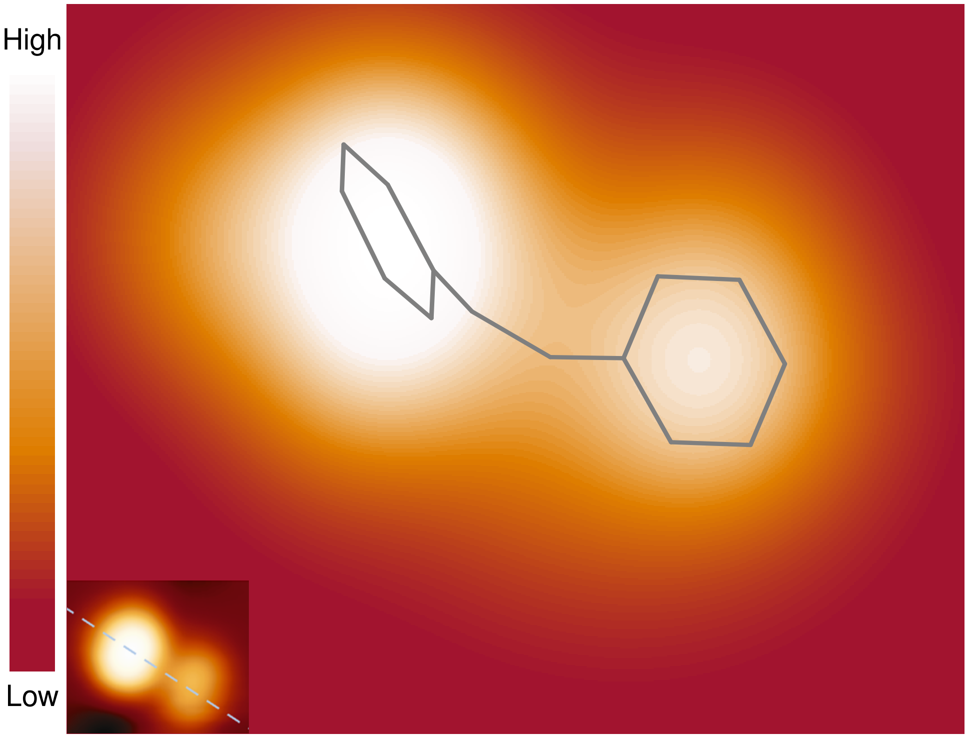

Fig. S4 Calculated STM image with the positive sample bias 1.0 V for *cis*-down configuration, and the experimental STM image extracted from Ref. 19 is inset.

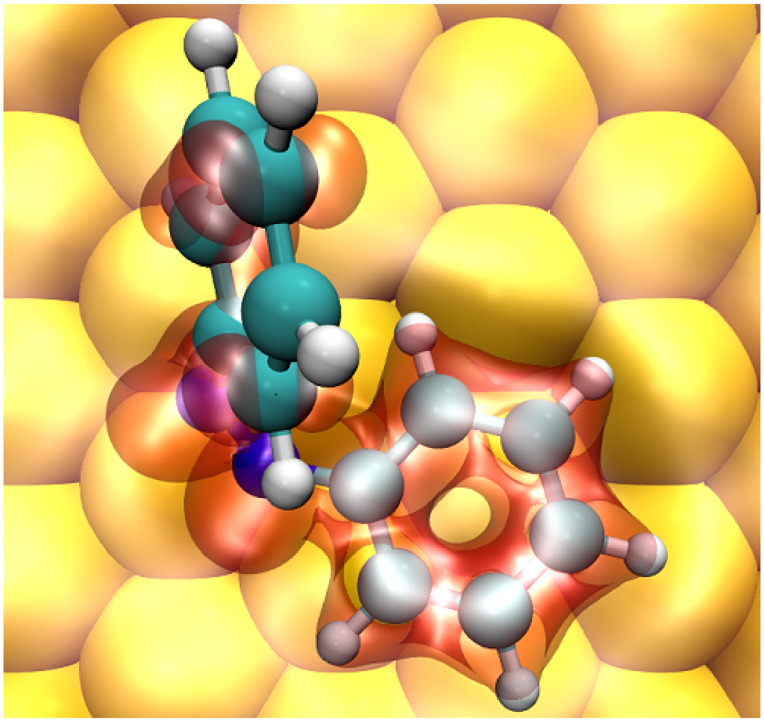

Fig. S5 Isosurface with the value of 0.001 e/Å^3 (red) of the density of states under experimental positive 1.0 V sample bias for *cis*-para molecule adsorbed on the Au(111) surface.

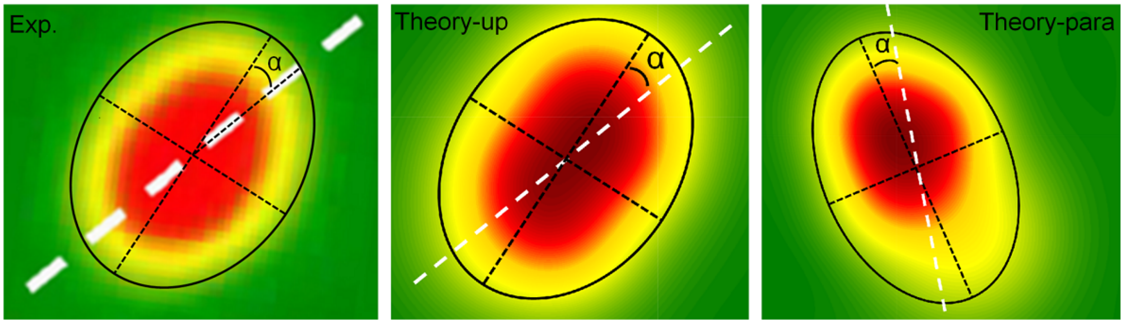

Fig. S6 The fitting of ellipse shape with experimental STM image (Exp., left), calculated *cis*-up STM image (Theory-up, middle) and *cis*-para STM image (Theory-para, right). The dashed white line is used for the corresponding STM height profile measurement in the main text. α is the angle between the major axis of the ellipse and the dashed white line. The experimental STM image and the dashed white line used for STM height measurement (Exp., left) are extracted from Ref. 14.

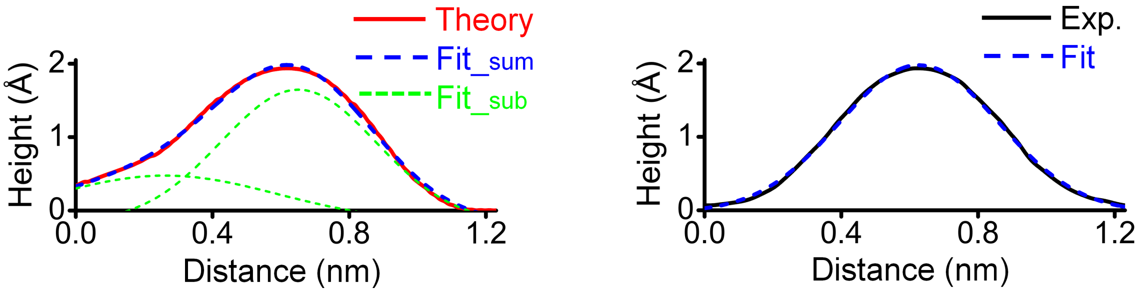

Fig. S7 The fitting line (blue dash line, Fit$_{sum}$) and its two components (green short dash lines, Fit$_{sub}$) mimicked by Gaussian functions, comparing to the calculated STM height profile for *cis*-para configuration (red solid line, theory) in the left panel. The fitting line (blue dash line, Fit) mimicked by a single Gaussian function, comparing to the experimental STM height profile for *cis*-isomer (black solid line, Exp.) in the right panel. The experimental height profile is extracted from Ref. 14.

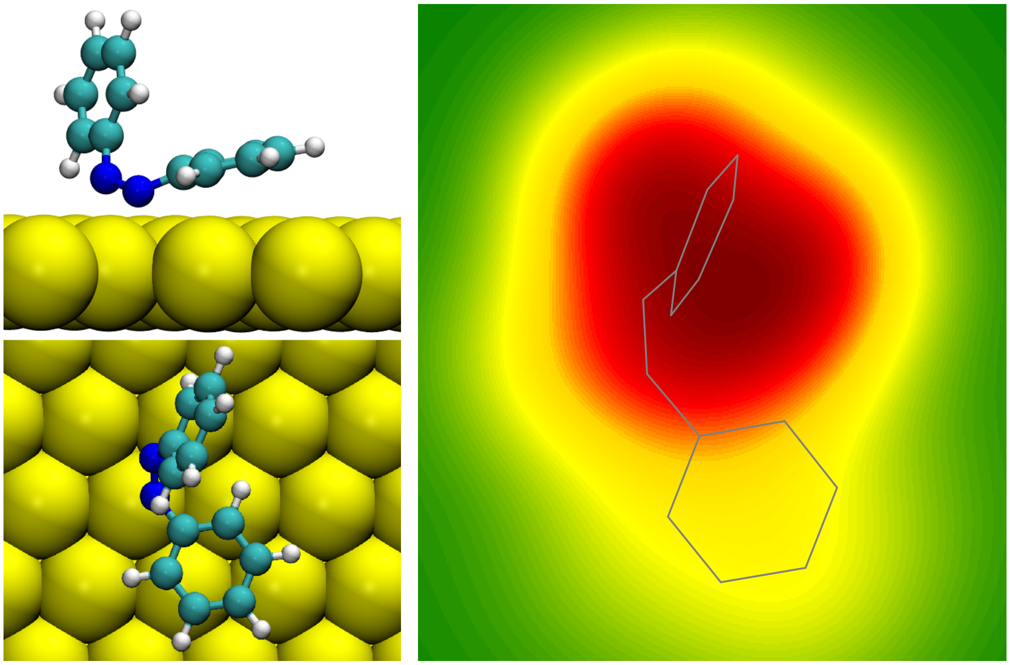

Fig. S8 Optimized stable *cis*-configuration of azobenzene molecule adsorbed on Au(111) surface in side and top views (left panel) as well as the accordingly calculated STM image with the positive sample bias 1.0 V under the same experimental conditions[14] (right panel).

Table S2 Parameters used in Gaussian function to fit the theoretical STM height profiles for *cis*-para and *cis*-up as well as the experimental measurement for *cis* configuration adsorbed on Au(111). Specifically, $\mathrm{Fit_{sub1}}$ and $\mathrm{Fit_{sub2}}$ in *cis*-para are accordant to the low peak and high peak in green short dash lines (left, in Fig. S7), respectively, Fit in *cis*-up is accordant to the blue dash line of Fig. S10, and Fit in Exp. is accordant to the blue dash line (right, in Fig. S7).

	cis-para		*cis*-up	Exp.
	$\mathrm{Fit_{sub1}}$	$\mathrm{Fit_{sub2}}$	Fit	Fit
y_0	−0.1638	− 0.1638	−0.1952	−0.0260
a	0.4947	0.9661	1.4615	1.1039
w	0.7733	0.5337	0.6136	0.5495
b	0.2625	0.6511	0.6289	0.6276

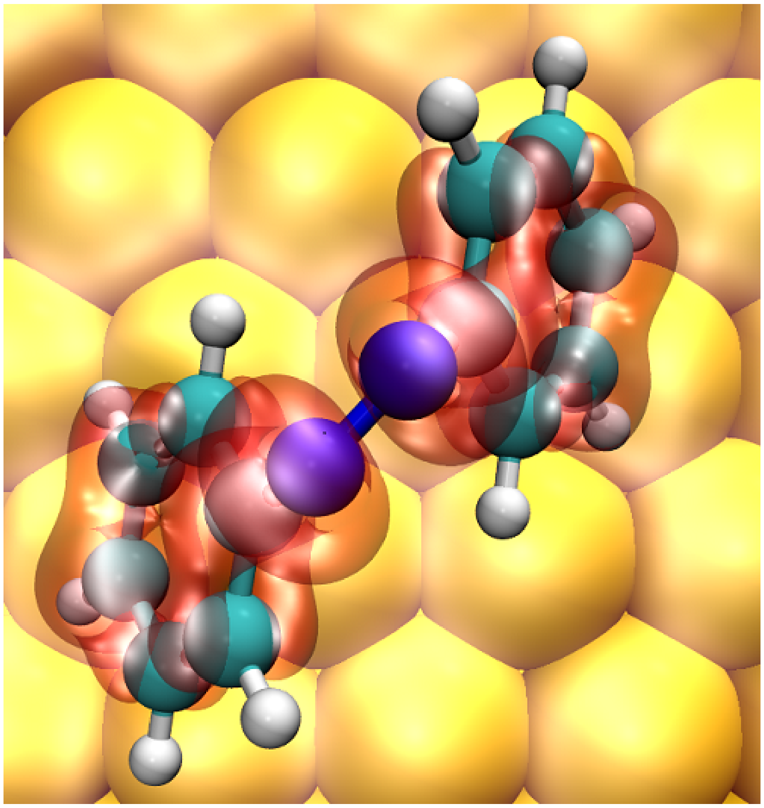

Fig. S9 Isosurface with the value of 0.002 e/Å^3 (red) of the density of states under experimental positive 1.0 V sample bias for *cis*-up molecule adsorbed on the Au(111) surface.

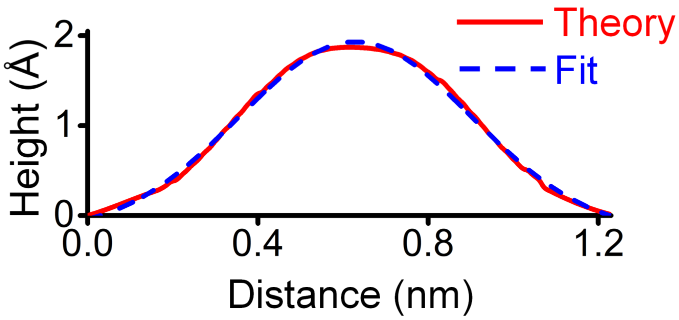

Fig. S10 The fitting line (blue dash line, Fit) mimicked by a single Gaussian function, comparing to the calculated STM height profile for *cis*-up configuration (red solid line, theory).

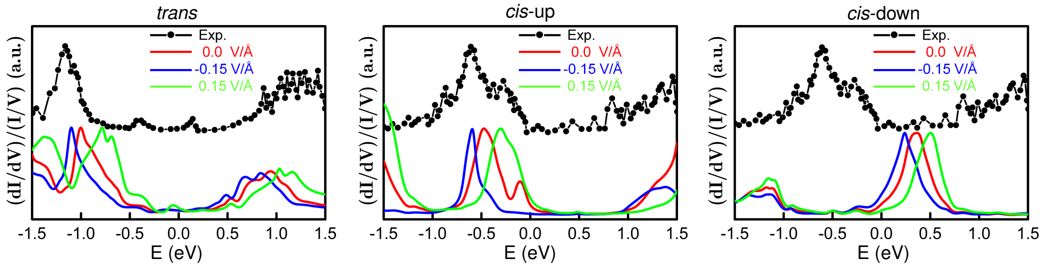

Fig. S11 The theoretical (solid line) and experimental (black solid circle) scanning tunneling spectroscopy (STS) spectra for *trans* (left), *cis*-up (middle) and *cis*-down (right). The red, blue and green solid lines represent the theoretical STS without electric field effects, with a -0.15 V/Å and 0.15 V/Å electric fields, respectively. The -0.15 V/Å (0.15 V/Å) accords with the experimental negative (positive) bias voltage of 1.5 V in Ref. 14. The experimental STS spectra are extracted from Ref. 14.

S4 Electric field effects

Table S3 The electric field effects on the relative stabilities of the configurations with respect to *trans* for an electric field of -0.1 V/Å and 0.1 V/Å. Here a positive electric field points upward from Au(111) to AB molecule, which equals a positive sample bias. The single-point energy was calculated based on the configurations without an electric field. The magnitude of 0.15 V/Å accords with the experimental bias voltage of 1.5 V (assuming a 10 Å sample-tip distance) in Ref. 14.

	0.0 V/Å	-0.1 V/Å	-0.15 V/Å	0.1 V/Å	0.15 V/Å
trans	0.000	0.000	0.000	0.000	0.000
TS1	1.113	1.146	1.160	1.073	1.046
cis – down	0.826	0.905	0.938	0.747	0.703
cis – para	1.112	1.174	1.195	1.038	0.999
TS2	1.896	1.802	1.781	1.921	1.929
cis – up	1.305	1.224	1.184	1.386	1.411

S5 Binding energies

Table S4 Calculated binding energies E_{bin} of different configurations adsorbed on Au(111).

	E_{bin} in eV
trans	1.663
cis – down	1.340
cis – para	1.049
cis – up	0.878

References

1 G. Kresse and J. Furthmüller, *Phys. Rev. B*, 1996, **54**, 11169–11186.
2 J. P. Perdew, K. Burke and M. Ernzerhof, *Phys. Rev. Lett.*, 1996, **77**, 3865–3868.
3 P. E. Blöchl, O. Jepsen and O. K. Andersen, *Phys. Rev. B*, 1994, **49**, 16223–16233.
4 G. Kresse and D. Joubert, *Phys. Rev. B*, 1999, **59**, 1758–1775.
5 S. Grimme, J. Antony, S. Ehrlich and H. Krieg, *J. Chem. Phys.*, 2010, **132**, 154104.
6 S. Grimme, S. Ehrlich and L. Goerigk, *J. Comput. Chem.*, 2011, **32**, 1456–1465.
7 D. R. Lide, *Handbook of Chemistry and Physics, 87th ed.*, CRC press, 2004.
8 H. J. Monkhorst and J. D. Pack, *Phys. Rev. B*, 1976, **13**, 5188–5192.
9 J. Neugebauer and M. Scheffler, *Phys. Rev. B*, 1992, **46**, 16067–16080.
10 G. Makov and M. C. Payne, *Phys. Rev. B*, 1995, **51**, 4014–4022.
11 J. Tersoff and D. R. Hamann, *Phys. Rev. B*, 1985, **31**, 805–813.
12 A. D. Gottlieb and L. Wesoloski, *Nanotechnology*, 2006, **17**, R57.
13 W. A. Hofer, A. S. Foster and A. L. Shluger, *Rev. Mod. Phys.*, 2003, **75**, 1287–1331.
14 B.-Y. Choi, S.-J. Kahng, S. Kim, H. Kim, H. W. Kim, Y. J. Song, J. Ihm and Y. Kuk, *Phys. Rev. Lett.*, 2006, **96**, 156106.
15 R. M. Feenstra, *Phys. Rev. B*, 1991, **44**, 13791–13794.
16 G. Henkelman, B. P. Uberuaga and H. Jónsson, *J. Chem. Phys.*, 2000, **113**, 9901–9904.
17 C. J. Chen, *Phys. Rev. Lett.*, 1992, **69**, 1656–1659.
18 S. Heinze, *Appl. Phys. A*, 2006, **85**, 407–414.
19 N. Henningsen, R. Rurali, K. Franke, I. Fernández-Torrente and J. Pascual, *Appl. Phys. A*, 2008, **93**, 241.